

# Atom diode: Variants, stability, limits, and adiabatic interpretation

A. Ruschhaupt\* and J. G. Muga†

*Departamento de Química-Física, Universidad del País Vasco, Apdo. 644, 48080 Bilbao, Spain*

We examine and explain the stability properties of the “atom diode”, a laser device that lets the ground state atom pass in one direction but not in the opposite direction. The diodic behavior and the variants that result by using different laser configurations may be understood with an adiabatic approximation. The conditions to break down the approximation, which imply also the diode failure, are analyzed.

PACS numbers: 03.75.Be, 42.50.Lc

## I. INTRODUCTION

In a previous paper [1] we proposed simple models for an “atom diode”, a laser device that lets the neutral atom in its ground state pass in one direction (conventionally from left to right) but not in the opposite direction for a range of incident velocities. A diode is a very basic control element in a circuit, so many applications may be envisioned to trap or cool atoms, or to build logic gates for quantum information processing in atom chips or other setups. Similar ideas have been developed independently by Raizen and coworkers [2, 3]. While their work has emphasized phase space compression, we looked for the laser interactions leading to the most effective diode. This lead us to consider first STIRAP [4] (stimulated Raman adiabatic passage) transitions and three level atoms, although we also proposed schemes for two-level atoms. In this paper we continue the investigation on the atom diode, concentrating on its two-level version, by examining its stability with respect to parameter changes, and also several variants, including in particular the ones discussed in [1] and [2]. We shall see that the behaviour of the diode, its properties, and its working parameter domain can be understood and quantified with the aid of an adiabatic basis (equivalently, partially dressed states) obtained by diagonalizing the effective interaction potential.

We restrict the atomic motion, similarly to [1], to one dimension. This occurs when the atom travels in waveguides formed by optical fields [5], or by electric or magnetic interactions due to charged or current-carrying structures [6]. It can be also a good approximation in free space for atomic packets which are broad in the laser direction, perpendicular to the incident atomic direction [7]. Three dimensional effects should not imply a dramatic disturbance, in any case, as we shall analyze elsewhere.

The basic setting can be seen in Fig. 1, and consists of three, partially overlapping laser fields: two of them are state-selective mirror lasers blocking the excited ( $|2\rangle$ ) and ground ( $|1\rangle$ ) states on the left and right, respectively

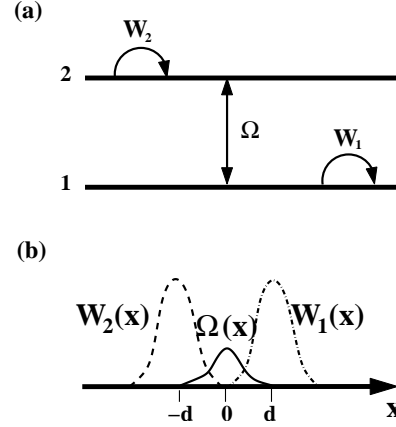


FIG. 1: (a) Schematic action of the different lasers on the atom levels and (b) location of the different laser potentials.

of a central pumping laser on resonance with the atomic transition. They are all assumed to be traveling waves perpendicular to the atomic motion direction. The corresponding effective, time-independent, interaction-picture Hamiltonian for the two-level atom may be written, using  $|1\rangle \equiv \begin{pmatrix} 1 \\ 0 \end{pmatrix}$  and  $|2\rangle \equiv \begin{pmatrix} 0 \\ 1 \end{pmatrix}$ , as

$$\mathbf{H} = \frac{\hat{p}_x^2}{2m} + \underbrace{\frac{\hbar}{2} \begin{pmatrix} W_1(x) & \Omega(x) \\ \Omega(x) & W_2(x) \end{pmatrix}}_{\mathbf{M}(x)}, \quad (1)$$

where  $\Omega(x)$  is the Rabi frequency for the resonant transition and the effective reflecting potentials are  $W_1(x)\hbar/2$  and  $W_2(x)\hbar/2$ .  $\hat{p}_x = -i\hbar\frac{\partial}{\partial x}$  is the momentum operator and  $m$  is the mass (corresponding to Neon in all numerical examples).

Spontaneous decay is neglected here for simplicity, but it could be incorporated following [1]. It implies both perturbing and beneficial effects for unidirectional transmission. Notice that in the ideal diode operation the ground state atom must be excited during its left-to-right crossing of the device. In principle, excited atoms could cross the diode “backwards”, i.e., from right to left, but an irreversible decay from the excited state to the ground state would block any backward motion [1].

The behaviour of this device is quantified by the scat-

\*Email address: wtxruxxa@lg.ehu.es

†Email address: jg.muga@ehu.es

tering transmission and reflection amplitudes for left (l) and right (r) incidence. Using  $\alpha$  and  $\beta$  to denote the channels,  $\alpha = 1, 2$ ,  $\beta = 1, 2$ , let us denote by  $R_{\beta\alpha}^l(v)$  ( $R_{\beta\alpha}^r(v)$ ) the scattering amplitudes for incidence with modulus of velocity  $v > 0$  from the left (right) in channel  $\alpha$ , and reflection in channel  $\beta$ . Similarly we denote by  $T_{\beta\alpha}^l(v)$  ( $T_{\beta\alpha}^r(v)$ ) the scattering amplitude for incidence in channel  $\alpha$  from the left (right) and transmission in channel  $\beta$ .

For some figures, it will be preferable to use an alternative notation in which the information of the superscript (l/r) is contained instead in the sign of the velocity argument  $w$ , positive for left incidence and negative otherwise,

$$R_{\beta\alpha}(w) := \begin{cases} R_{\beta\alpha}^l(|w|), & \text{if } w > 0 \\ R_{\beta\alpha}^r(|w|), & \text{if } w < 0 \end{cases}$$

$$T_{\beta\alpha}(w) := \begin{cases} T_{\beta\alpha}^l(|w|), & \text{if } w > 0 \\ T_{\beta\alpha}^r(|w|), & \text{if } w < 0 \end{cases}$$

The ideal diode configuration must be such that

$$|T_{21}^l(v)|^2 \approx |R_{11}^r(v)|^2 \approx 1, \quad (2)$$

$$|R_{\beta 1}^l(v)|^2 \approx |T_{\beta 1}^r(v)|^2 \approx |R_{21}^r(v)|^2 \approx |T_{11}^l(v)|^2 \approx 0, \quad (3)$$

with  $\beta = 1, 2$ , in an interval  $v_{min} < v < v_{max}$  of the modulus of the velocity. In words, there must be full transmission for left incidence and full reflection for right incidence in the ground state. This was achieved in [1] with a particular choice of the potential in which  $\Omega(x)$ ,  $W_1(x)$ , and  $W_2(x)$  were related to two partially overlapping functions  $f_1(x)$ ,  $f_2(x)$ . However, other forms are also possible, so we shall deal here with the more general structure of Eq. (1). We shall use Gaussian laser profiles

$$W_1(x) = \hat{W}_1 \Pi(x, d), \quad W_2(x) = \hat{W}_2 \Pi(x, -d),$$

$$\Omega(x) = \hat{\Omega} \Pi(x, 0),$$

where

$$\Pi(x, x_0) = \exp[-(x - x_0)^2 / (2\Delta x^2)]$$

and  $\Delta x = 15 \mu\text{m}$ .

In section II we shall examine the stability and limits of the “diodic” behavior while the variants of the atom diode are presented in section III. They are explained in section IV with the aid of an adiabatic basis and approximation. The paper ends with a summary and an appendix on the adiabaticity criterion.

## II. “DIODIC” BEHAVIOUR AND ITS LIMITS

The behavior of the two-level atom diode is examined by solving numerically the stationary Schrödinger equation,

$$E_v \Psi(x) = \mathbf{H} \Psi(x), \quad (4)$$

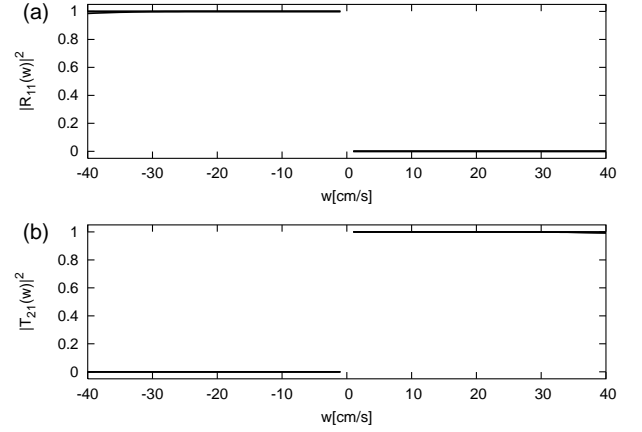


FIG. 2: (a) Reflection probability  $|R_{11}(w)|^2$  and (b) transmission probability  $|T_{21}(w)|^2$ ; recall that in this notation  $w < 0$  corresponds to incidence from the right, and  $w > 0$  to incidence from the left;  $d = 50 \mu\text{m}$ ;  $\hat{\Omega} = 1 \times 10^6/\text{s}$ ,  $\hat{W}_1 = \hat{W}_2 = 100 \times 10^6/\text{s}$ ;  $\hat{\Omega} = 0.2 \times 10^6/\text{s}$ ,  $\hat{W}_1 = 20 \times 10^6/\text{s}$ ,  $\hat{W}_2 = 100 \times 10^6/\text{s}$ ;  $\hat{\Omega} = 0.2 \times 10^6/\text{s}$ ,  $\hat{W}_1 = 100 \times 10^6/\text{s}$ ,  $\hat{W}_2 = 20 \times 10^6/\text{s}$  (coinciding solid lines).

with the Hamiltonian given by Eq. (1) and  $E_v = \frac{m}{2}v^2$ . The results, obtained by the “invariant imbedding method” [8, 9], are shown in Fig. 2 for different parameters. In the plotted velocity range, the “diodic” behaviour holds, i.e. Eqs. (2) and (3) are fulfilled. (The transmission and reflection probabilities for incidence in the ground state,  $|R_{21}^{l/r}|^2$  and  $|T_{11}^{l/r}|^2$ , which are not shown in the Figure are zero.) The device may be asymmetric, i.e. even with  $\hat{W}_1 \neq \hat{W}_2$  there can be a “diodic” behaviour, see some examples in Fig. 2.

Note in passing that the device works as a diode for incidence in the excited state too, but in the opposite direction, namely,  $|T_{12}^r(v)|^2 \approx |R_{22}^l(v)|^2 \approx 1$ , whereas all other probabilities for incidence in the excited state are approximately zero.

Now let us examine the stability of the diode with respect to changes in the separation between laser field centers  $d$ . We define  $v_{max}$  and  $v_{min}$  as the upper and lower limits where diodic behaviour holds, by imposing that all scattering probabilities from the ground state be small except the ones in Eq. (2) (i.e., the transmission probability from 1 to 2 for left incidence and the reflection probability from 1 to 1 for right incidence). More precisely,  $v_{max/min}$  are chosen as the limiting values such that  $\sum_{\beta=1}^2 (|R_{\beta 1}^l|^2 + |T_{\beta 1}^r|^2) + (|R_{21}^r|^2 + |T_{11}^l|^2) + (1 - |T_{21}^l|^2) + (1 - |R_{11}^r|^2) < \epsilon$  for all  $v_{min} < v < v_{max}$ . In Fig. 3,  $v_{max/min}$  are plotted versus the distance between the laser centers,  $d$ , for different combinations of  $\hat{\Omega}$ ,  $\hat{W}_1$ , and  $\hat{W}_2$ . For the intensities considered,  $v_{max}$  is in the ultra-cold regime below 1 m/s. In the  $v_{max}$  surface, unfilled boxes indicate reflection failure for right incidence and filled circles indicate transmission failure for left in-

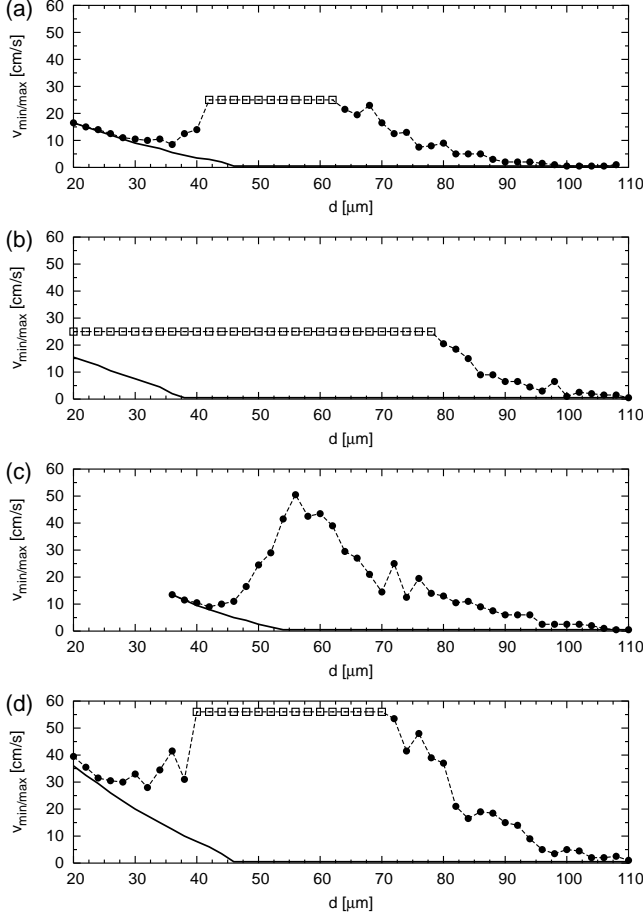


FIG. 3: Limit  $v_{min}$  (solid lines) and  $v_{max}$  (symbols connected with dashed lines) for “diodic” behaviour,  $\epsilon = 0.01$ ; the circles (boxes) correspond to breakdown due to transmission (reflection); (a)  $\hat{\Omega} = 0.2 \times 10^6/\text{s}$ ,  $\hat{W}_1 = \hat{W}_2 = 20 \times 10^6/\text{s}$ ; (b)  $\hat{\Omega} = 1 \times 10^6/\text{s}$ ,  $\hat{W}_1 = \hat{W}_2 = 20 \times 10^6/\text{s}$ ; (c)  $\hat{\Omega} = 0.2 \times 10^6/\text{s}$ ,  $\hat{W}_1 = \hat{W}_2 = 100 \times 10^6/\text{s}$ ; (d)  $\hat{\Omega} = 1 \times 10^6/\text{s}$ ,  $\hat{W}_1 = \hat{W}_2 = 100 \times 10^6/\text{s}$ .

cidence. In the  $v_{min}$  surface, the failure is always due to transmission failure for left incidence. We see that the valid  $d$  range for “diodic” behaviour can be increased by increasing the Rabi frequency  $\hat{\Omega}$ , compare e.g. (a) and (b), or (c) and (d). Moreover, higher mirror intensities increase  $v_{max}$  at the plateau but also make it narrower, compare e.g. (b) and (d). This narrowing can be simply compensated by increasing  $\hat{\Omega}$  too, compare e.g. (a) and (d).

Finally, we have also examined the stability with respect to a shift  $\Delta$  of the central position of the pumping laser, see Fig. 4. It turns out that there is a range, which depends on  $d$ , where the limits  $v_{min}$  and  $v_{max}$  practically do not change.

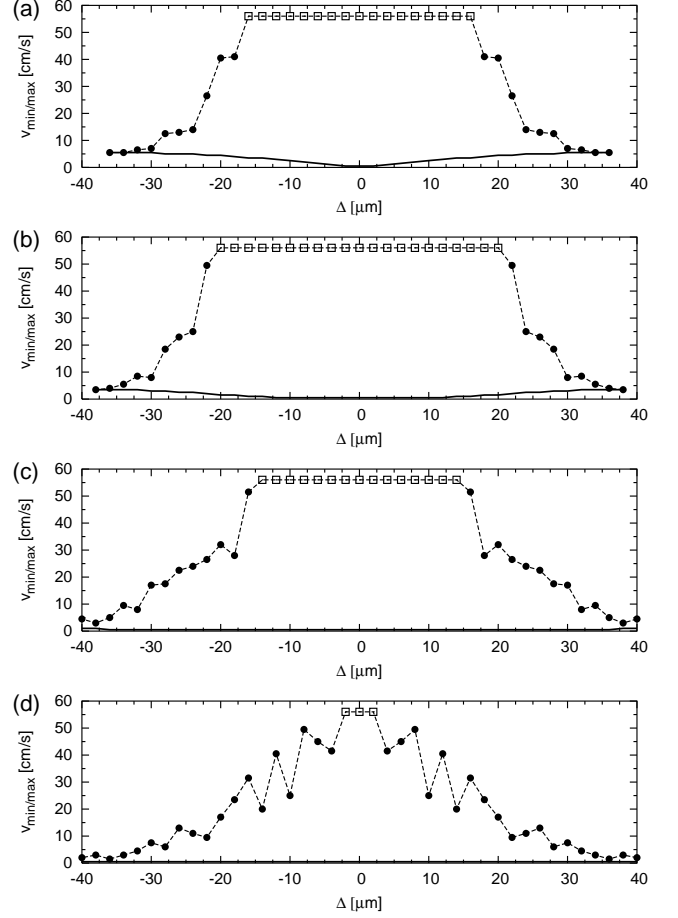


FIG. 4: Limit  $v_{min}$  (solid lines) and  $v_{max}$  (symbols connected with dashed lines) for “diodic” behaviour versus the shift  $\Delta$  for different  $d$ ,  $\epsilon = 0.01$ ; the circles (boxes) correspond to breakdown first for transmission (reflection);  $\hat{\Omega} = 1 \times 10^6/\text{s}$ ,  $\hat{W}_1 = \hat{W}_2 = 100 \times 10^6/\text{s}$ ; (a)  $d = 46 \mu\text{m}$ , (b)  $d = 50 \mu\text{m}$ , (c)  $d = 60 \mu\text{m}$ , (d)  $d = 70 \mu\text{m}$ .

### III. VARIANTS OF THE ATOM DIODE

Is the mirror potential  $W_2$  really necessary? If we want ground state atoms to pass from left to right but not from right to left, it is not intuitively obvious why we should add a reflection potential for the excited state on the left of the pumping potential  $\Omega$ , see again Fig. 1. In other words, it could appear that the pumping potential and a reflecting potential  $W_1$  on its right would be enough to make a perfect diode. This simpler two-laser scheme, however, only works partially. In Fig. 5 the scattering probabilities for the case  $\hat{W}_1 > 0$ ,  $\hat{W}_2 = 0$  are represented. While there is still full reflection if the atom comes from the right, the transmission probability is only 1/2 when the atom comes from the left; accordingly there is a 1/2 reflection probability from the left, which is equally distributed between the ground and excited state channels. This is in contrast to the  $\hat{W}_1 > 0$ ,

$\hat{W}_2 > 0$  case of Fig 2. We may thus conclude that the counterintuitive state-selective mirror  $W_2$  is really important to attain a perfect diode.

In Fig. 5 the case  $\hat{W}_1 = 0$ ,  $\hat{W}_2 > 0$  is also plotted. For incidence from the right in the ground state there is no full reflection so this case is not useful as a diode. But for incidence from the left there is equal transmission in ground and excited states so that this device might be useful to build an interferometer. A very remarkable and useful property in this case, and in fact in all cases depicted in Figs. 2 and 5, is the constant value of the transmission and reflection probabilities in a broad velocity range. This is calling for an explanation. Moreover, why do they take the values 1, 1/2, or 1/4? None of these facts is very intuitive, neither within the representations and concepts we have put forward so far, nor according to the following arguments: Let us consider again the simple two-laser configuration with  $\hat{W}_2 = 0$  and  $\hat{W}_1 > 0$ . From a classical perspective, the atom incident from the left finds first the pumping laser and then the state-selective mirror potential for the ground state. According to this “sequential” model, one would expect an important effect of the velocity in the pumping efficiency. A different velocity implies a different traversal time and thus a different final phase for the Rabi oscillation which should lead to a smooth, continuum variation of the final atomic state with the velocity. In particular, the probability of the excited state after the pumping would oscillate with the velocity and therefore the final transmission after the right mirror should oscillate too, if the sequential model picture were valid. Indeed, these oscillations are clearly seen in Fig. 6 when  $\hat{W}_1 = \hat{W}_2 = 0$  (above a low velocity threshold in which the Rabi oscillations are suppressed and all channels are equally populated, for a related effect see [10], see also the explanation of this low velocity regime in section IV). Clearly, however, the oscillations are absent when  $\hat{W}_1 > 0$ , so the sequential, classical-like picture cannot be right. In summary, the mirror potentials added to the pumping laser imply a noteworthy stabilization of the probabilities and velocity independence. The failure of the sequential scattering picture must be due to some sort of quantum interference phenomenon. Interference effects are well known in scattering off composite potentials, but in comparison with, e.g., resonance peaks in a double barrier, the present results are of a different nature. There is indeed a clean explanation to all the mysteries we have dropped along the way as the reader will find out in the next section.

#### IV. ADIABATIC INTERPRETATION OF THE DIODE AND ITS VARIANTS

Depending on the mirror potentials included in the device, let us label the four possible cases discussed in the previous section as follows: case “0”:  $\hat{W}_1 = \hat{W}_2 = 0$ ; case “1”:  $\hat{W}_1 > 0$ ,  $\hat{W}_2 = 0$ ; case “2”:  $\hat{W}_1 = 0$ ,  $\hat{W}_2 > 0$ ; case “12”:  $\hat{W}_1 > 0$ ,  $\hat{W}_2 > 0$ . We diagonalize now the

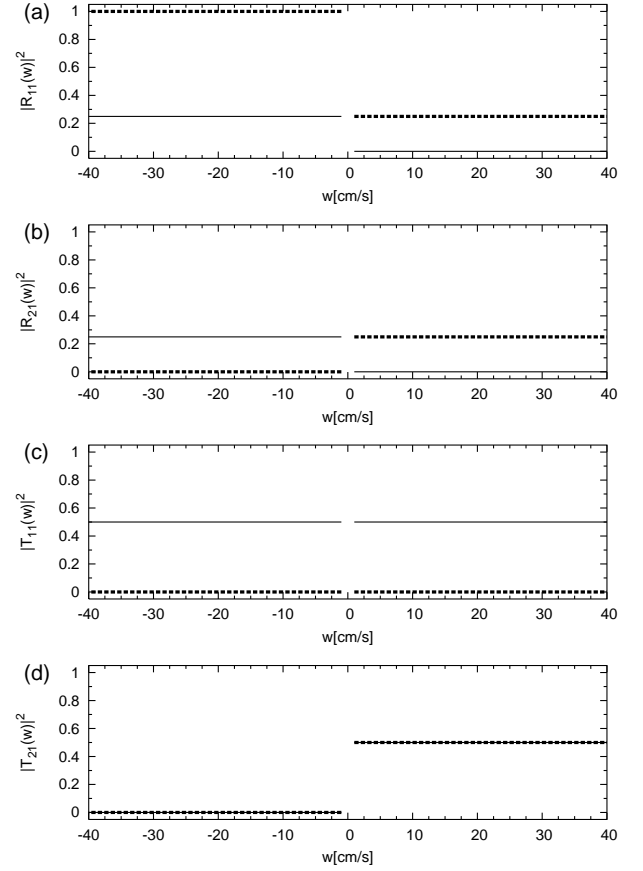


FIG. 5: (a) Reflection probability  $|R_{11}(w)|^2$ , (b) reflection probability  $|R_{21}(w)|^2$ , (c) transmission probability  $|T_{11}(w)|^2$ ; (d) transmission probability  $|T_{21}(w)|^2$ ;  $d = 50 \mu\text{m}$ ,  $\hat{\Omega} = 1 \times 10^6/\text{s}$ ;  $\hat{W}_1 = 100 \times 10^6/\text{s}$ ,  $\hat{W}_2 = 0$  (dashed lines);  $\hat{W}_1 = 0$ ,  $\hat{W}_2 = 100 \times 10^6/\text{s}$  (solid lines).

potential matrix  $\mathbf{M}(x)$

$$\mathbf{U}(x)\mathbf{M}(x)\mathbf{U}^\dagger(x) = \begin{pmatrix} \lambda_-(x) & 0 \\ 0 & \lambda_+(x) \end{pmatrix}.$$

The orthogonal matrix  $\mathbf{U}(x)$  is given by

$$\mathbf{U}(x) = \begin{pmatrix} \frac{W_-(x) - \mu(x)}{\sqrt{4\Omega^2(x) + [W_-(x) - \mu(x)]^2}} & \frac{W_-(x) + \mu(x)}{\sqrt{4\Omega^2(x) + [W_-(x) + \mu(x)]^2}} \\ \frac{2\Omega(x)}{\sqrt{4\Omega^2(x) + [W_-(x) - \mu(x)]^2}} & \frac{2\Omega(x)}{\sqrt{4\Omega^2(x) + [W_-(x) + \mu(x)]^2}} \end{pmatrix}$$

where

$$W_- = W_1 - W_2, \\ \mu = \sqrt{4\Omega^2(x) + W_-^2(x)},$$

and the eigenvalues of  $\mathbf{M}(x)$  are

$$\lambda_\mp(x) = \frac{\hbar}{4} [W_1(x) + W_2(x) \mp \mu(x)]$$

with corresponding (normalized) eigenvectors  $|\lambda_\mp(x)\rangle$ . The asymptotic form of  $\mathbf{U}$  varies for the different cases

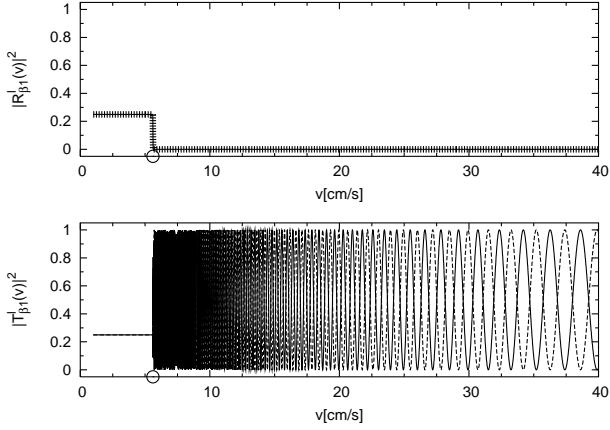


FIG. 6: Reflection and transmission probability for incidence from the left,  $d = 50 \mu\text{m}$ ,  $\hat{\Omega} = 1 \times 10^6/\text{s}$ ,  $\hat{W}_1 = \hat{W}_2 = 0$ ; the circles indicate  $v_{\lambda, \max}$  while in this case  $v_{\lambda, \min} = 0$  (see Eqs. (7) and (8)); (a)  $|R_{11}^l(v)|^2$  (thick dotted line),  $|R_{21}^l(v)|^2$  (solid line); (b)  $|T_{11}^l(v)|^2$  (dashed line),  $|T_{21}^l(v)|^2$  (solid line).

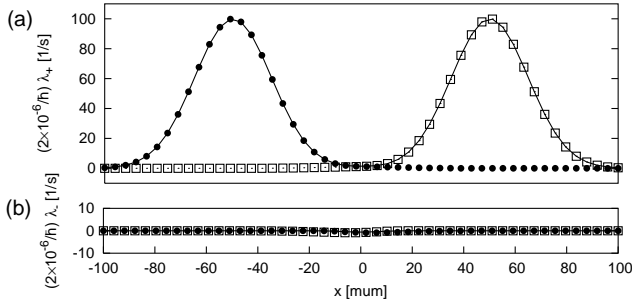


FIG. 7: Eigenvalues (a)  $\lambda_+$  and (b)  $\lambda_-$ ;  $d = 50 \mu\text{m}$ ,  $\hat{\Omega} = 1 \times 10^6/\text{s}$ ;  $\hat{W}_1 = \hat{W}_2 = 100 \times 10^6/\text{s}$  (solid lines);  $\hat{W}_1 = 100 \times 10^6/\text{s}$ ,  $\hat{W}_2 = 0$  (boxes);  $\hat{W}_1 = 0$ ,  $\hat{W}_2 = 100 \times 10^6/\text{s}$  (circles).

distinguished with a superscript,  $U^{(j)}$ ,  $j = 0, 1, 2, 12$ . For  $x \rightarrow -\infty$ , the same  $U$  is found for cases 0 and 1, in which the left edge corresponds to the pumping potential. Similarly, the cases 2 and 12 share the same left edge potential  $W_2$  and thus a common form of  $U$ ,

$$U^{(0,1)}(-\infty) = \frac{1}{\sqrt{2}} \begin{pmatrix} -1 & 1 \\ 1 & 1 \end{pmatrix}, \quad U^{(2,12)}(-\infty) = \begin{pmatrix} -1 & 0 \\ 0 & 1 \end{pmatrix}.$$

The corresponding analysis for  $x \rightarrow \infty$  gives the asymptotic forms

$$U^{(0,2)}(\infty) = \frac{1}{\sqrt{2}} \begin{pmatrix} -1 & 1 \\ 1 & 1 \end{pmatrix}, \quad U^{(1,12)}(\infty) = \begin{pmatrix} 0 & 1 \\ 1 & 0 \end{pmatrix}.$$

The eigenvalues  $\lambda_{\pm}(x)$  for the same parameters of Fig. 5 are plotted in Fig. 7. We see that  $\lambda_+(x) > 0$  has at least one high barrier whereas  $\lambda_-(x) \approx 0$ .

If  $\Psi$  is a two-component solution of the stationary

Schrödinger equation, Eq. (4), we define now the vector

$$\Phi(x) = \begin{pmatrix} \phi_-(x) \\ \phi_+(x) \end{pmatrix} := U(x)\Psi(x)$$

in a potential-adapted, “adiabatic representation”. Note that if no approximation is made,  $\Phi$  and  $\Psi$  are both exact and contain the same information expressed in different bases. Starting from Eq. (4), using  $\Psi = U^+ \Phi$ , and multiplying from the left by  $U$ , we arrive at the following equation for  $\Phi(x)$

$$E_v \Phi(x) = -\frac{\hbar^2}{2m} \frac{\partial^2}{\partial x^2} \Phi(x) + \begin{pmatrix} \lambda_-(x) & 0 \\ 0 & \lambda_+(x) \end{pmatrix} \Phi(x) + Q \Phi(x),$$

where

$$Q = -\frac{\hbar^2}{2m} \left( U(x) \frac{\partial^2 U^+}{\partial x^2}(x) + 2U(x) \frac{\partial U^+}{\partial x}(x) \frac{\partial}{\partial x} \right) = \begin{pmatrix} m B^2(x)/2 & -A(x) + iB(x)\hat{p}_x \\ A(x) - iB(x)\hat{p}_x & m B^2(x)/2 \end{pmatrix} \quad (5)$$

is the coupling term in the adiabatic basis, and  $A(x)$ ,  $B(x)$  are real functions,

$$A(x) = \frac{1}{32\mu^4(x)\Delta x^4 m} \left\{ \exp\left(-\frac{(x+d)^2}{\Delta x^2}\right) d^2 \hbar^6 \Omega(x) W_-(x) + \exp\left(\frac{(x+d)^2}{\Delta x^2}\right) \times \right. \\ \left. [-4\Omega^2(x) + W_1^2(x) + W_2^2(x) + 6W_1(x)W_2(x)] \right\},$$

$$B(x) = \frac{d\hbar^3}{4\mu^2(x)\Delta x^2 m} \Omega(x) [W_1(x) + W_2(x)].$$

Let us consider incidence from the left and assume first that the coupling  $Q$  can be neglected so that there are two independent adiabatic modes ( $\pm$ ) in which the internal state of the atom adapts to the position-dependent eigenstates  $|\lambda_{\pm}\rangle$  of the laser potential  $M$ , whereas the atom center-of-mass motion is affected in each mode by the effective adiabatic potentials  $\lambda_{\pm}(x)$ .

Because  $\lambda_- \approx 0$ , an approximate solution for  $\phi_-(x)$  is a full transmitted wave and because  $\lambda_+$  consists of at least one “high” barrier—at any rate the present argument is only applicable for energies below the barrier top—, an approximate solution for  $\phi_+(x)$  is a wave which is fully reflected by a wall. So we can write for  $x \ll 0$ ,

$$\Phi(x) \approx \Phi_{-\infty}(x) := \begin{pmatrix} c_- \\ c_+ \end{pmatrix} e^{ikx} + \begin{pmatrix} 0 \\ -c_+ \end{pmatrix} e^{-ikx},$$

and for  $x \gg 0$ ,

$$\Phi(x) \approx \Phi_{\infty}(x) := \begin{pmatrix} c_- \\ 0 \end{pmatrix} e^{ikx}.$$

TABLE I: Reflection and transmission probability for the different variations of the atom diode

(a) incidence from the right:

case	$c_-^r$	$c_+^r$	$R_{11}^r$	$R_{21}^r$	$T_{11}^r$	$T_{21}^r$
(0) $\hat{W}_1 = \hat{W}_2 = 0$	$-\frac{1}{\sqrt{2}}$	$\frac{1}{\sqrt{2}}$	$-\frac{1}{2}$	$-\frac{1}{2}$	$\frac{1}{2}$	$-\frac{1}{2}$
(1) $\hat{W}_1 > 0, \hat{W}_2 = 0$	0	1	-1	0	0	0
(2) $\hat{W}_1 = 0, \hat{W}_2 > 0$	$-\frac{1}{\sqrt{2}}$	$\frac{1}{\sqrt{2}}$	$-\frac{1}{2}$	$-\frac{1}{2}$	$\frac{1}{\sqrt{2}}$	0
(12) $\hat{W}_1 > 0, \hat{W}_2 > 0$	0	1	-1	0	0	0

(b) incidence from the left:

case	$c_-^l$	$c_+^l$	$R_{11}^l$	$R_{21}^l$	$T_{11}^l$	$T_{21}^l$
(0) $\hat{W}_1 = \hat{W}_2 = 0$	$-\frac{1}{\sqrt{2}}$	$\frac{1}{\sqrt{2}}$	$-\frac{1}{2}$	$-\frac{1}{2}$	$\frac{1}{2}$	$-\frac{1}{2}$
(1) $\hat{W}_1 > 0, \hat{W}_2 = 0$	$-\frac{1}{\sqrt{2}}$	$\frac{1}{\sqrt{2}}$	$-\frac{1}{2}$	$-\frac{1}{2}$	0	$-\frac{1}{\sqrt{2}}$
(2) $\hat{W}_1 = 0, \hat{W}_2 > 0$	-1	0	0	0	$\frac{1}{\sqrt{2}}$	$-\frac{1}{\sqrt{2}}$
(12) $\hat{W}_1 > 0, \hat{W}_2 > 0$	-1	0	0	0	0	-1

In order to determine the amplitudes  $c_{\pm}$  we have to compare with the asymptotic form of the scattering solution for left incidence,

$$\Psi(x) \approx \Psi_{-\infty}(x) := \begin{pmatrix} 1 \\ 0 \end{pmatrix} e^{ikx} + \begin{pmatrix} R_{11}^l \\ R_{21}^l \end{pmatrix} e^{-ikx}$$

if  $x \ll 0$  and

$$\Psi(x) \approx \Psi_{\infty}(x) := e^{ikx} \begin{pmatrix} T_{11}^l \\ T_{21}^l \end{pmatrix}$$

if  $x \gg 0$ .

The transmission and reflection coefficients can now be approximately calculated for each case from the boundary conditions  $\Phi_{-\infty}(x) = U(-\infty)\Psi_{-\infty}(x)$  and  $\Phi_{\infty}(x) = U(\infty)\Psi_{\infty}(x)$ .

The incidence from the right can be treated in a similar way. All the amplitudes are given in Table I, from which we can find, taking the squares, the transmission and reflection probabilities 1, 1/2, 1/4, and 0, of Figs. 2, 5, and 6.

These results provide in summary a simple explanation of the behaviour of the diode and its variants. In particular, the perfect diode behavior of case 12, occurs because the (approximately) “freely” moving mode  $\phi_-$  transfers adiabatically the ground state to the excited state from left to right. To visualize this, let us represent the probabilities to find the ground and excited state in the eigenvectors  $|\lambda_{\pm}^{(j)}(x)\rangle$  for the cases  $j = 12, 1$ . They are plotted in Fig. 8a for the case “12”: the perfect adiabatic transfer can be seen clearly. On the other hand, the mode “+” (not plotted), which tends to the ground state on the right edge of the device, is blocked by a high barrier. The stability of this blocking effect with respect to incident velocities holds for energies smaller than the  $\lambda_+$  barrier top, more on this below. In Fig. 8b

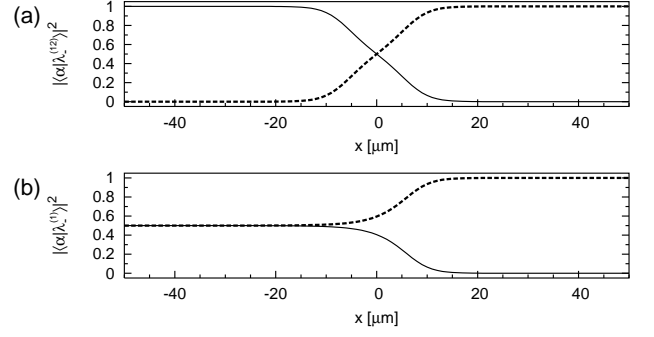


FIG. 8:  $|\langle 1|\lambda_{-}^{(j)}\rangle|^2$  (solid lines) and  $|\langle 2|\lambda_{-}^{(j)}\rangle|^2$  (dashed lines) for  $d = 50 \mu\text{m}$ ,  $\hat{\Omega} = 1 \times 10^6/\text{s}$ ,  $\hat{W}_1 = 100 \times 10^6/\text{s}$ ; (a)  $\hat{W}_2 = 100 \times 10^6/\text{s}$  (case  $j = 12$ ), (b)  $\hat{W}_2 = 0$  (case  $j = 1$ ).

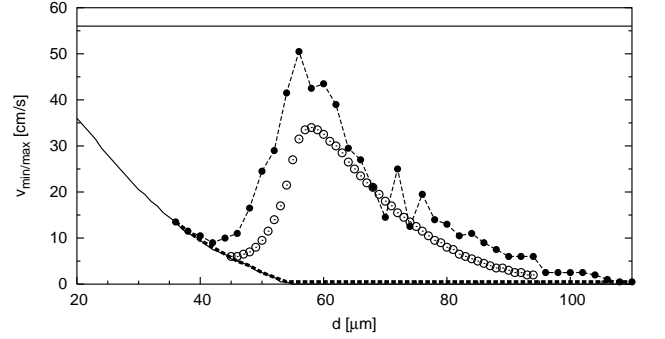


FIG. 9: Limits of the “diodic” behaviour  $v_{min}$  (thick dashed line) and  $v_{max}$  (filled circles connected with a dashed line, see also Fig. 3),  $\epsilon = 0.01$ ; limits of condition (6)  $v_{\lambda,min}$  (lower solid line) and  $v_{\lambda,max}$  (upper solid line); limit of the adiabatic approximation  $v_{ad,max}$  (unfilled circles),  $\epsilon = 0.01$ ;  $\hat{W}_1 = \hat{W}_2 = 100 \times 10^6/\text{s}$ ,  $\hat{\Omega} = 0.2 \times 10^6/\text{s}$ .

the ground and excited state probabilities for case “1” are plotted. If the mirror potential laser  $W_2$  is removed on the left edge of the device, the ground state is not any more an eigenstate of the potential for  $x \ll 0$ . The adiabatic transfer of the mode “−” occurs instead from  $(|2\rangle - |1\rangle)/2^{1/2}$  on the left to  $|2\rangle$  on the right, whereas the blocked mode “+” on the left corresponds to the linear combination  $(|2\rangle + |1\rangle)/2^{1/2}$ . This results in a 1/2 reflection probability for ground-state incidence from the left. A similar analysis would be applicable in the other cases.

Of course all approximations have a range of validity that depend on the potential parameters and determines the working conditions of the diode. Even though these conditions can be easily found numerically from the exact results, approximate breakdown criteria are helpful to understand the limits of the device and different reasons for its failure.

For the approximation that  $\phi_-$  is a fully transmitted wave and  $\phi_+$  a fully reflected one a necessary condition

is

$$\max_x [\lambda_-(x)] < E_v < \max_x [\lambda_+(x)]. \quad (6)$$

This defines the limits

$$v_{\lambda,min} := \sqrt{\frac{2}{m} \max_x [\lambda_-(x)]}, \quad (7)$$

$$v_{\lambda,max} := \sqrt{\frac{2}{m} \max_x [\lambda_+(x)]}, \quad (8)$$

such that Eq. (6) is fulfilled for all  $v$  with  $v_{\lambda,min} < v < v_{\lambda,max}$ . The plateaus of  $v_{max}$  seen e.g. in Fig. 3 for a range of  $d$ -values are essentially coincident with  $v_{\lambda,max}$ . Fig. 9 shows the exact limits  $v_{min}$  and  $v_{max}$  for the “diodic” behaviour, as in Fig. 3c, and also the limits  $v_{\lambda,min}$ ,  $v_{\lambda,max}$  resulting from the condition of Eq. (6). We see that the exact limit  $v_{min}$  coincides essentially with  $v_{\lambda,min}$  so that the lower “diodic” velocity boundary can be understood by the breakdown of the condition that  $\phi_-$  is fully transmitted due to a  $\lambda_-$  barrier. This effect is only relevant for small distances  $d$  between the lasers.

Another reason for the breaking down of the diode may be that the adiabatic modes are no longer independent, i.e. that  $\mathbf{Q}$ , see Eq. (5), cannot be neglected. An approximate criterion for adiabaticity, more precisely for neglecting the non-diagonal elements of  $\mathbf{Q}$ , see the Appendix, is

$$q(v) := \max_{x \in I} \frac{|A(x)|^2 + 2m |B(x)|^2 [E_v - \lambda_-(x)]}{|\lambda_+(x) - \lambda_-(x)|^2} \ll 1 \quad (9)$$

with  $I = [-d, d]$ . A velocity boundary  $v_{ad,max}$  defined by  $q(v) < \epsilon$  for all  $v_{\lambda,min} < v < v_{ad,max}$  is shown in Fig. 9. (Note that the condition of Eq. (9) only makes sense if  $E_v > \lambda_-(x)$ , i.e.  $v_{\lambda,min} < v$ .) We see in Fig. 9 that the breakdown of the diode at  $v_{max}$  for large  $d$  is due to a failure of the adiabatic approximation.

## V. SUMMARY

Summarizing, we have studied a two-level model for an “atom diode”, a laser device in which ground state atoms can pass in one direction, conventionally from left to right, but not in the opposite direction. The proposed scheme includes three lasers: two of them are state-selective mirrors, one for the excited state on the left, and the other one for the ground state on the right, whereas the third one -located between the two mirrors- is a pumping laser on resonance with the atomic transition.

We have shown that the “diodic” behaviour is very stable with respect to atom velocity in a given range, and with respect to changes in the distances between the centers of the lasers. The inclusion of the laser on the left,

reflecting the excited state, is somewhat counterintuitive, but it is essential for a perfect diode effect; the absence of this laser leads to a 50% drop in efficiency. The stability properties as well as the actual mechanism of the diode is explained with an adiabatic basis and an adiabatic approximation. The diodic transmission is due to the adiabatic transfer of population from left to right, from the ground state to the excited state in a free-motion adiabatic mode, while the other mode is blocked by a barrier.

## Acknowledgments

AR acknowledges support by the Ministerio de Educación y Ciencia. This work has been supported by Ministerio de Educación y Ciencia (BFM2003-01003), and UPV-EHU (00039.310-15968/2004).

## APPENDIX A

To motivate Eq. (9), see also [11], let us assume

$$E\Phi(x) = -\frac{\hbar^2}{2m} \frac{\partial^2}{\partial x^2} \Phi(x) + \begin{pmatrix} \lambda_- & 0 \\ 0 & \lambda_+ \end{pmatrix} \Phi(x) + \epsilon \begin{pmatrix} 0 & -\tilde{A} + i\tilde{B}\hat{p}_x \\ \tilde{A} - i\tilde{B}\hat{p}_x & 0 \end{pmatrix} \Phi(x) \quad (A1)$$

where  $\lambda_{\pm}$ ,  $\tilde{A}$  and  $\tilde{B}$  are real and independent of  $x$ . We assume that  $E > \lambda_-$  and that  $\epsilon$  is small such that we can treat  $\Phi$  perturbatively,

$$\Phi(x) \approx \begin{pmatrix} \phi_{0,-}(x) \\ \phi_{0,+}(x) \end{pmatrix} + \epsilon \begin{pmatrix} \phi_{1,-}(x) \\ \phi_{1,+}(x) \end{pmatrix}$$

with

$$\begin{aligned} \phi_{0,-}(x) &= \exp\left(\frac{i}{\hbar} \sqrt{2m(E - \lambda_-)} x\right) \\ \phi_{0,+}(x) &= 0 \end{aligned}$$

Then it follows from (A1) for the first-order correction

$$\begin{aligned} \phi_{1,-} &= 0 \\ \phi_{1,+} &= [E - \lambda_+ - \hat{p}_x^2/(2m)]^{-1} (\tilde{A} - i\tilde{B}\hat{p}_x) \phi_{0,-} \\ &= \frac{\tilde{A} - i\tilde{B}\sqrt{2m(E - \lambda_-)}}{\lambda_- - \lambda_+} \phi_{0,-} \end{aligned}$$

because  $\hat{p}_x \phi_{0,-} = \sqrt{2m(E - \lambda_-)} \phi_{0,-}$ . If we want to neglect  $\phi_+ = 0 + \epsilon \phi_{1,+}$  we get the condition

$$\epsilon^2 \frac{|\tilde{A}|^2 + |\tilde{B}|^2 2m(E - \lambda_-)}{|\lambda_- - \lambda_+|^2} \ll 1.$$

If  $\lambda_{\pm}$ ,  $\tilde{A}$  and  $\tilde{B}$  depend on  $x$ , we may use the condition

$$\max_{x \in I} \frac{|\epsilon \tilde{A}(x)|^2 + |\epsilon \tilde{B}(x)|^2 2m[E - \lambda_-(x)]}{|\lambda_-(x) - \lambda_+(x)|^2} \ll 1$$

where  $I$  is chosen in such a way that the assumption  $\phi_{0,+}(x) = 0$  is approximately valid.

In Eq. (A1), we have not included any diagonal elements in the coupling, compare with Eq. (5). We neglect them in the condition (9) but in principle it would be also possible to absorb them by defining effective adiabatic potentials  $\tilde{\lambda}_{\pm} = \lambda_{\pm} + mB^2/2$ .

- 
- [1] A. Ruschhaupt and J.G. Muga, Phys. Rev. A **70**, 061604(R) (2004).
  - [2] M.G. Raizen, A.M. Dudarev, Qian Niu, and N.J. Fisch, Phys. Rev. Lett. **94**, 053003 (2005).
  - [3] A.M. Dudarev, M. Marder, Qian Niu, N.J. Fisch and M.G. Raizen, Europhysics Letters to be published.
  - [4] K. Bergmann, H. Theuer, and B. W. Shore, Rev. Mod. Phys. **70**, 1003 (1998).
  - [5] D. Schneble, M. Hasuo, T. Anker, T. Pfau, and J. Mlynek, J. Opt. Soc. Am. B **20**, 648 (2003).
  - [6] R. Folman, P. Krüger, J. Schmiedmayer, J. Denschlag, and C. Henkel, Advances in Atomic, Molecular, and Optical Physics **48**, 263 (2002).
  - [7] V. Hannstein, G. C. Hegerfeldt, J. G. Muga, J. Phys. B: At. Mol. Opt. Phys. **38**, 409 (2005).
  - [8] S. Singer, K.F. Freed, and Y.B. Band, J. Chem. Phys. **77**, 1942 (1982).
  - [9] Y.B. Band and I. Tuvi, J. Chem. Phys. **100**, 8869 (1994).
  - [10] B. Navarro, I. L. Egusquiza, J. G. Muga and G. C. Hegerfeldt, Phys. Rev. A **67**, 063819 (2003).
  - [11] A. Messiah, *Quantum Mechanics* (Wiley, New York, 1958).